Proc. Natl. Acad. Sci. USA
Vol. 76, No. 12, pp. 6042–6046, December 1979
Chemistry

Structure of carboxymyoglobin in crystals and in solution

(heme–ligand coordination geometry/heme proteins/infrared spectroscopy/iron–carbonyl/protein structure)

MARVIN W. MAKINEN†, ROBERT A. HOUTCHENS‡, AND WINSLOW S. CAUGHEY‡

†Department of Biophysics and Theoretical Biology, Cummings Life Science Center, The University of Chicago, Chicago, Illinois 60637; and ‡Department of Biochemistry, Colorado State University, Fort Collins, Colorado 80523

Communicated by Martin Karplus, September 10, 1979

ABSTRACT **The configuration of the heme–carbonyl group upon binding of carbon monoxide to sperm whale myoglobin (Mb) in crystals is evaluated on the basis of infrared spectroscopic methods. Multiplets of the totally symmetric C-O stretching mode are observed for the heme-bound ligand near 1933, 1944, and 1967 cm^{-1}, corresponding to three different heme–carbonyl conformers. Variations in the relative proportions of these conformers can be induced by incorporation of small fractions of metMb or deoxyMb into MbCO crystals. The configuration of the iron–carbonyl with respect to the immediate coordination environment of the heme iron is assigned for each ν(CO) stretching frequency on the basis of a detailed comparison of the three-dimensional structures of the heme environments of MbCO, metMb, and deoxyMb defined by crystallographic methods. The structures of the three heme–carbonyl conformers account for the ν(CO) infrared absorption bands that can be observed for MbCO in solution.**

The three-dimensional structures of carbon monoxide (CO)-liganded hemoglobins (Hbs) and myoglobins (Mbs) (1–5) exhibit a bent or tilted configuration of the CO ligand with respect to the porphyrin ring, whereas small-molecule model CO-liganded heme complexes (6, 7) exhibit a perpendicular linear (Fe—Ĉ—O) bonding structure. The origin of the different configuration in heme proteins is attributed primarily to nonbonding steric interactions of the axial ligand with nearby amino acid residues. The assumption is generally made that the heme-carbonyl configuration of heme proteins in crystals is identical to that in solution. It is well known, nonetheless, that the infrared (IR) absorption spectrum of sperm whale carboxymyoglobin (MbCO) in solution is indicative of two structurally distinguishable components (8, 9), although only one configuration is identified in the crystal by neutron diffraction data (3).

In recent studies of the polarized single crystal absorption spectra of Mb complexes (10, 11), we have detected differences in the configuration of the heme-carbonyl group induced by crystal environment and have demonstrated that the single-crystal spectrum of MbCO formed under conditions comparable to those in neutron diffraction studies (3) is not quantitatively compatible with the spectrum of MbCO in solution. In this communication we report the results of investigations in which we have extended these observations by application of IR spectroscopic methods. We provide evidence on the basis of the IR absorption of MbCO in crystals that three structurally distinct heme-carbonyl conformers arising from changes in nearest neighbor intermolecular interactions in the crystal can be identified on the basis of the ν(CO) stretching frequency. The structural origin of the ν(CO) stretching frequencies indicative of each conformer is explained on the basis of the three-dimensional structure of sperm whale Mb (3, 12, 13) determined by crystallographic methods. The results suggest that structural changes in the immediate environment of the iron-carbonyl group may occur as a function of the occupancy of ligand binding sites in the crystal.

EXPERIMENTAL

Sperm whale metmyoglobin (metMb) obtained from Sigma was crystallized (14) in space groups $P2_1$ and $P2_12_12_1$. For conversion to the MbCO derivative, the crystals were washed as required with protein-free solutions of either concentrated ammonium sulfate or phosphate at neutral pH and were reduced with sodium dithionite under anaerobic conditions followed by overnight equilibration with CO at 1 atmosphere (101 kPa) pressure. Manipulation of crystals was carried out with use of a microscope kept in a small plastic bag inflated with CO. Small platelets and crystal fragments (longest dimension $\leq$0.1 mm) were selected and deposited uniformly over the optical surface of a CaF_2 window of an IR cell (pathlength 0.14 mm). Excess solvent was removed by blotting with strips of filter paper prior to assembling the cell, and the spectra were recorded with the sample maintained at $\approx$0°C in a Perkin–Elmer 180 spectrometer interfaced to a Tektronix 4051 computer for data acquisition (15, 16). Electronic absorption spectra in the visible range were recorded with a Cary 17 spectrometer directly with the crystalline or solution sample of MbCO in the IR cell.

Evaluation of the nonbonding van der Waals interactions of the heme-carbonyl group with nearby protein residues was made on the basis of atomic model building studies carried out with aid of the molecular graphics display system and programs of R. J. Feldmann (17) at the National Institutes of Health. For this purpose the refined atomic coordinates of MbCO at 2.0-Å resolution obtained from neutron diffraction studies (B. P. Schoenborn and J. C. Hanson, personal communication) and of metMb and deoxyMb (12, 13), similarly obtained by x-ray data at 2.0-Å resolution, were employed.

RESULTS

IR absorption spectra of sperm whale MbCO in solution are illustrated in Fig. 1. In the upper part of Fig. 1 the spectrum of MbCO is identical to that described by McCoy and Caughey (8). The most prominent ν(CO) absorption is characteristically observed at 1944 cm^{-1} with a shoulder near 1933 cm^{-1}, while a weak band is observed under conditions of high signal-to-noise ratio near 1967 cm^{-1}. Previous investigations (8, 9) have established that the relative intensities of the bands near 1944 and

The publication costs of this article were defrayed in part by page charge payment. This article must therefore be hereby marked "*advertisement*" in accordance with 18 U. S. C. §1734 solely to indicate this fact.

Abbreviations: CO, carbon monoxide; deoxyMb, deoxymyoglobin; IR, infrared; Mb, myoglobin; MbCO, carboxymyoglobin; MbO_2, oxymyoglobin; metMb, metmyoglobin; for corresponding hemoglobin derivatives, the Mb is replaced by Hb.

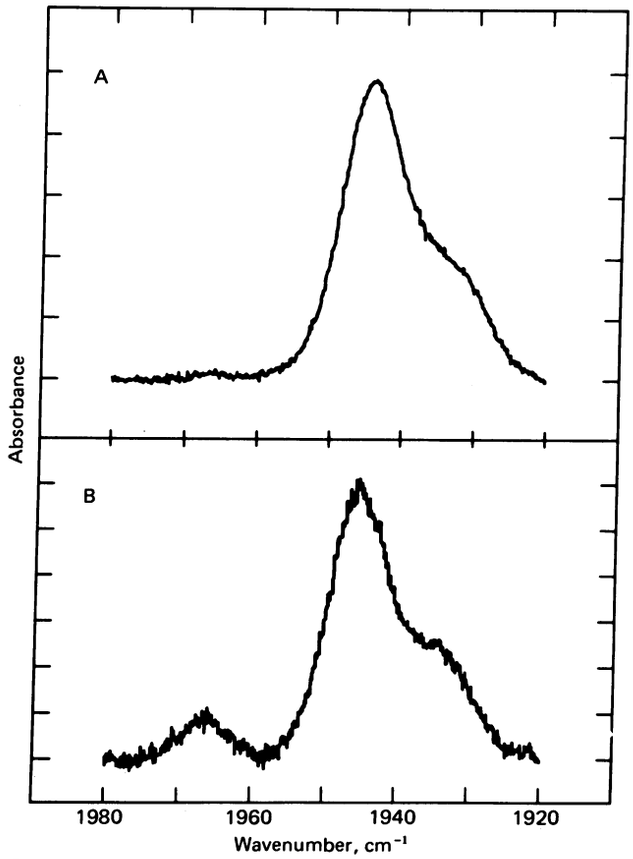

FIG. 1. IR spectra in the C-O stretch region of solutions of sperm whale Mb. (*A*) Spectrum of a solution consisting of MbCO (≈0.002 M) prepared by dissolving crystals of MbCO of space group $P2_12_12_1$ with nitrogen-saturated dilute phosphate buffer (pH ≈7). (*B*) Spectrum of a solution of MbCO (≈0.002 M) in the presence of ≈0.009 M $ZnSO_4$ buffered to pH 7 with 0.005 M Tris·HCl buffer. In each case, an IR cell with CaF_2 windows having a pathlength of 0.05 mm was employed.

1933 cm^{-1} remain essentially constant in the pH 5–9 range, whereas more recent studies (18) reveal only slight shifts in the relative intensities of the 1967, 1944, and 1933 cm^{-1} bands with a change in temperature between 0°C and 30°C.

As illustrated in the lower part of Fig. 1, the component absorbing near 1967 cm^{-1} is more prominent for MbCO in the presence of Zn^{2+}. Absorption near 1967 cm^{-1} has been frequently associated with a denatured form of the protein because acid denaturation of MbCO (9) and HbCO (19) gives rise to a broad ($\Delta\nu_{1/2} \approx 15$ cm^{-1}) absorption band in this region. However, binding of Zn^{2+} to Mb in solution, under conditions comparable to those described in Fig. 1*B*, results in increased affinity for CO binding (20). In Fig. 1*B* the band near 1967 cm^{-1} is narrower than that generally observed upon acid denaturation, and the components near 1944 and 1933 cm^{-1} are better resolved with no change in their relative intensities. These features indicate that the appearance of the 1967 cm^{-1} component is not due to the denaturant action of Zn^{2+}. Similarly, it has been demonstrated (4, 21) that the CO-liganded forms of Hb Zürich and Hb Sidney exhibit intense bands near 1968 cm^{-1} not attributable to denatured forms of the protein.

The results of previous investigations (10, 11) have demonstrated that the spectroscopic properties of MbCO in crystals indicative of changes in heme–carbonyl configuration are dependent upon the presence of oxidized Mb incorporated into the crystal structure. Here we have extended those studies by developing methods to "dope" selectively metMb or deoxyMb into crystals of MbCO as a means of perturbing the heme–carbonyl group of MbCO molecules through their crystal environment. The extent of the incorporation of metMb or deoxyMb was estimated on the basis of the visible absorption spectrum of MbCO crystals. When MbCO crystals placed on the IR cell windows were bathed in a solution containing ≈0.01 M sodium dithionite under a CO atmosphere for several hours in the dark, metMb or deoxyMb were not detected. On the other hand, equilibration of MbCO crystals washed with a nitrogen-saturated buffer but without added dithionite resulted in the appearance of metMb, as evidenced by weak absorption near 500 and 630 nm. Equilibration of MbCO crystals with dithionite in a nitrogen-saturated buffer during irradiation from microscopic white light produced crystals containing deoxyMb, as evidenced by increased absorption near 555 nm and in the far visible region. Although by spectral criteria the crystals consisted predominantly of MbCO, variable fractions (≈15–30%) of metMb or deoxyMb could be incorporated into the crystals in this manner. Similar results were obtained for both monoclinic and orthorhombic crystals, and the IR spectra were dependent only upon the absence of or the incorporation of metMb or deoxyMb into the crystals. We assume that the doping of MbCO crystals with metMb or deoxyMb occurs according to a statistically random distribution.

The IR absorption spectra of MbCO in crystals are compared in Fig. 2. The spectrum of MbCO in crystals is quantitatively compatible with the spectrum of MbCO in solution only under conditions of incorporation of metMb into the crystal structure. This spectrum, as illustrated in the upper part of Fig. 2, exhibits the characteristic prominent ν(CO) absorption at 1944 cm^{-1}, the less intense shoulder near 1933 cm^{-1}, and a minor contribution near 1967 cm^{-1}. The relative intensities of all three components are comparable to those in the spectrum of MbCO in solution illustrated in Fig. 1*A*. Correspondingly, the polarized single crystal absorption spectrum of MbCO in crystals containing metMb (10, 11) is quantitatively compatible with the spectrum of MbCO in solution in the 250- to 600-nm range.

The spectrum of crystals composed of only MbCO is illustrated in Fig. 2*B*. In contrast to the results in Fig. 2*A*, the spectrum shows a reversal of the relative intensities of the absorption bands at 1944 and 1933 cm^{-1}. Additionally, the weakly absorbing species near 1967 cm^{-1} is essentially absent. Although the relative height of the 1933 cm^{-1} band is greatly increased with respect to that at 1944 cm^{-1}, we have not found conditions under which the component absorbing at 1944 cm^{-1} is totally absent. The reversal in the relative band heights can mean only that the species absorbing near 1933 cm^{-1} has become the predominant conformer. It is evident that the spectrum in Fig. 2*B* is not quantitatively compatible with the spectrum of MbCO in solution (Fig. 1*A*). Correspondingly, the polarized single crystal absorption spectrum of MbCO formed under identical conditions is not quantitatively compatible with the spectrum of MbCO in solution (11).

The IR spectrum of MbCO crystals containing deoxyMb is illustrated in Fig. 2*C*. Whereas the relative intensities of the ν(CO) absorption near 1944 and 1933 cm^{-1} remain comparable to those in Fig. 2*B*, there is an increase in the intensity of the weakly absorbing component near 1967 cm^{-1}. The half-band-width of the 1967-cm^{-1} component appears comparable to that in Fig. 1*B*. The appearance of the band at 1967 cm^{-1} in Fig. 2*C* indicates that the incorporation of deoxyMb into the crystal structure results in a relative increase in the fraction of the conformer in the crystal that gives rise to this absorption. These results stand in contrast to those in Fig. 1*B*, in which there is an increase in the intensity of the 1967 cm^{-1} band with retention of the characteristic solution ratios of the 1944 and 1933 cm^{-1} bands.

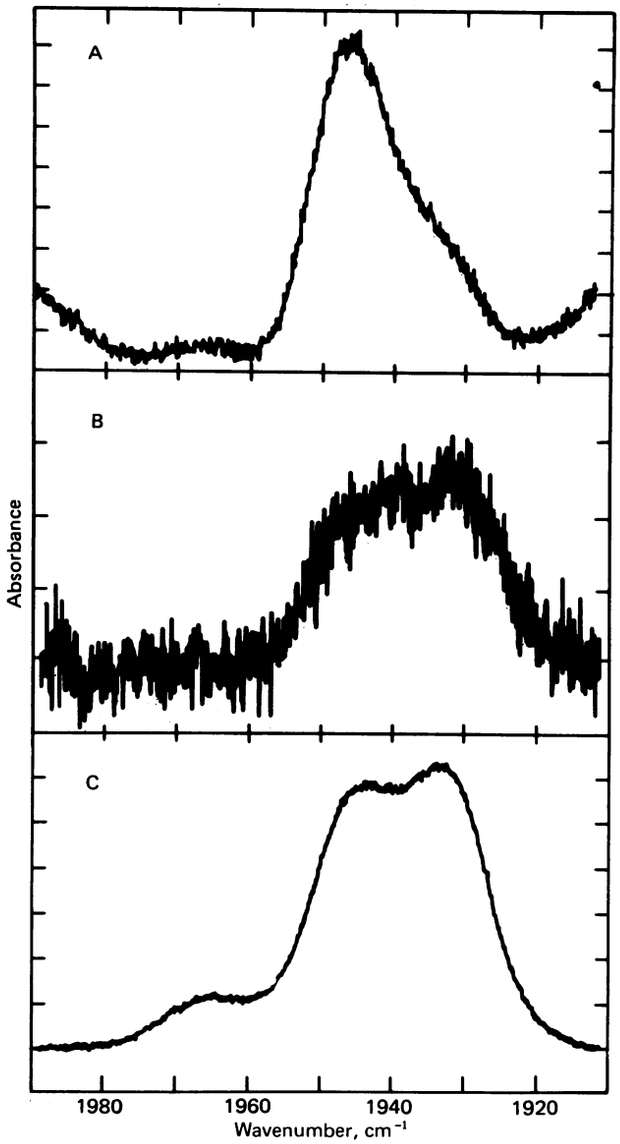

FIG. 2. IR spectra of sperm whale MbCO in crystals. Crystals were prepared as described in the text. (*A*) Crystals of MbCO containing ≈15–30% metMb in space group $P2_1$; comparable results were obtained with orthorhombic crystals. The curvature at the extreme ends of the spectrum is caused by background contributions of the ammonium sulfate solution. (*B*) Crystals of space group $P2_12_12_1$ containing only MbCO with no detectable metMb or deoxyMb; similar results but with a lower signal-to-noise ratio were obtained with monoclinic crystals. (*C*) Crystals of MbCO in space group $P2_12_12_1$ containing ≈20% deoxyMb; similar results but with a lower signal-to-noise ratio were obtained with monoclinic crystals.

DISCUSSION

The similar results obtained with monoclinic and orthorhombic crystals of Mb indicate that the changes in the relative intensities of the ν(CO) bands are not the result of differences in crystal structure but rather reflect intrinsic molecular properties of MbCO. The problem of immediate interest is to assign the detailed stereochemistry of iron–carbonyl bonding for each of the three ν(CO) frequencies. For metal–carbonyl complexes there are no specific guidelines for deducing ligand configuration from the frequency of the CO absorption bands (22, 23). However, the frequency of the totally symmetric C-O stretching mode of terminal metal–carbonyls reflects the extent of metal d_π electron delocalization into the π^* orbital of the CO ligand. Therefore, the CO stretching frequency of metal–carbonyl complexes is directly dependent upon the immediate environment of the metal ion and the stereochemistry of metal–ligand bonding. On this basis, the ν(CO) bands observed for MbCO correspond to different local environments of the iron–carbonyl group and define three heme–carbonyl conformers. The changes in the relative intensities of the ν(CO) bands of MbCO in crystals induced through manipulation of crystal composition correspond to alterations in their relative proportions. The results of this study are, thus, analogous to investigations of the structures of model complexes in which conformational isomers have been detected on the basis of multiplets of the symmetric C-O stretching mode of terminal metal–carbonyl groups (24).

We have suggested (11) that the structural origins of different heme–carbonyl conformers in crystals derive from intermolecular interactions imposed by crystal structure. These interactions will be dependent upon the detailed molecular structure of "foreign" Mb derivatives that have been incorporated into the MbCO crystals. In this investigation the salient correlative observation is that the band at 1933 cm^{-1} is observed predominantly in crystals containing only MbCO; the band at 1944 cm^{-1} is observed predominantly in crystals containing metMb; and the relative intensity of the band at 1967 cm^{-1} is increased upon incorporation of deoxyMb into MbCO crystals. We suggest that metMb incorporated into the crystal will tend to force neighboring MbCO molecules to acquire the tertiary structural characteristics of metMb through crystal-induced interactions, whereas the presence of deoxyMb will tend to force neighboring MbCO molecules to acquire the structural characteristics of deoxyMb. Alternatively, these interactions will be different from those in a crystal comprised of only MbCO. We, furthermore, suggest that the protein structural changes are correspondingly transmitted to the immediate donor ligand environment of the heme iron.

On this basis, we evaluate the structural origins of the three ν(CO) bands according to the detailed stereochemical differences of the environment of the heme iron in MbCO (3), metMb (12), and deoxyMb (13). Neutron diffraction studies of MbCO indicate that the N_ϵ atom of the imidazole ring of the distal (E7) histidine is in van der Waals contact with the carbonyl C atom. In contrast, the same N_ϵ atom is hydrogen bonded to the heme-linked water molecule in metMb and is, therefore, shifted away from the position of the carbonyl C atom in MbCO. In deoxyMb the position of the E7 imidazole group corresponds to an even greater movement from the site of the carbonyl C atom. These changes in the position of the E7 imidazole group are also reflected in an increasing separation of the N_ϵ atom from atoms in the porphyrin plane. For instance, the distance of the distal imidazole N_ϵ atom from the nitrogen atom of pyrrole ring A,[§] on the opposite side of the CO ligand, is correspondingly ≈4.2, 4.5, and 4.9 Å in MbCO, metMb, and deoxyMb, as estimated from the refined atomic coordinate data. There are also stereochemical changes of the imidazole group of the proximal (F8) histidine with respect to the heme. In MbCO the N_ϵ—Fe bond is essentially perpendicular to the mean porphyrin plane, whereas in metMb the N_ϵ—Fe bond deviates ≈4° from the heme normal. In deoxyMb a translational shift of the proximal imidazole increases the deviation of the N_ϵ—Fe bond from the heme axis to ≈11° while the tilt of the imidazole group with respect to the porphyrin plane remains unchanged. Additionally, in metMb and deoxyMb, the plane of the pyrrole nitrogen atoms is inclined to that of the peripheral porphyrin carbon atoms by ≈4°.

To evaluate the structural changes near the heme with re-

[§] The atomic numbering scheme is described in ref. 12.

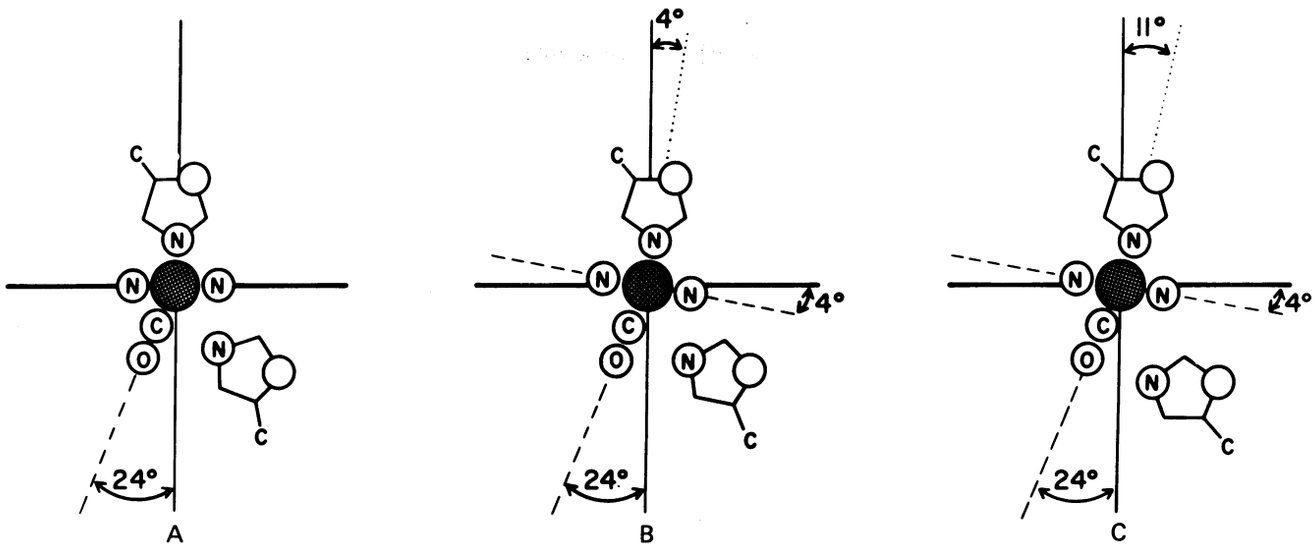

FIG. 3. Schematic illustration of structural changes in the immediate environment of the heme iron as assessed from model-building studies by comparison of the heme–carbonyl group in MbCO (*A*) to the environment of the group in metMb (*B*) and deoxyMb (*C*) to determine the stereochemical relationships of the proximal and distal imidazole groups to the iron–carbonyl unit. Conformations *A*, and *B*, and *C* are considered responsible for the 1933, 1944, and 1967 cm^{-1} bands, respectively, in the IR spectrum of MbCO. The change in tilt of the pyrrole nitrogen plane is expected by comparison of the detailed structural relationships described for the three derivatives on the basis of crystallographic studies. The diagrams are not drawn to scale according to atomic van der Waals radii, and the pyrrolic N—H group of the imidazole groups is represented by a circle. The iron atom is represented by the stippled circle, and the porphyrin plane by the horizontal straight line.

spect to the stereochemistry of the iron–carbonyl group, we have compared the environment of the heme–carbonyl group of MbCO to the environment of a heme–carbonyl group placed into the heme crevice of metMb and deoxyMb by use of computer-assisted molecular graphics techniques (17). This method of assessment of the heme crevice environment may be considered equivalent to model building studies in which the atomic model of a substrate is built into the active site region of an enzyme on the basis of the configuration of an inhibitor molecule determined by difference Fourier methods. Although the statistical significance of the structural differences of the three types of Mb derivatives is difficult to appraise objectively, especially for independently determined structures, the results depend only upon the feasibility of introducing a heme–carbonyl group into the heme crevice of the metMb and deoxyMb molecules with acceptable van der Waals contacts. On this basis, the model-building study requires assessment of the structural relationships of only the iron–carbonyl group with amino acid side chain residues and the pyrrole nitrogen atoms because the porphyrin skeleton remains essentially constant for all three derivatives.

The corresponding structures contributing to each ν(CO) absorption band are schematically illustrated in Fig. 3. The most prominent change concerns the relative position of the N_ϵ atom of the distal (E7) imidazole with respect to the ligand. In MbCO, interaction of the N_ϵ atom with the carbonyl C atom may be analogous to $sp \rightarrow \pi^*$ donation, an effect that would increase electron delocalization into the CO (π^*) orbitals (4, 15). The resultant effect would be a lowering of the ν(CO) stretching frequency. In the deoxyheme environment, the N_ϵ atom of the distal (E7) histidine is displaced and is found to be in van der Waals contact with the O atom. Displacement of the E7 imidazole N_ϵ atom from contact with the C atom would result in loss of these electronic interactions with a corresponding increase in ν(CO). For the metMb environment, the N_ϵ atom is intermediate between these two extreme positions. Furthermore, for structure 3*C*, the tilt of the plane of pyrrole nitrogens and the displacement of the N_ϵ atom of the proximal iron-coordinated imidazole ring, when viewed with reference to the iron–carbonyl group, suggest a straightening of the N_ϵ—Fe and Fe—C (carbonyl) bonds relative to each other.¶ This change results in closer approximation of octahedral coordination of the iron–carbonyl unit and is consistent with an increase in ν(CO) to 1967 cm^{-1} because model imidazole-coordinated heme–carbonyl complexes in solvents of low dielectric constant exhibit ν(CO) frequencies in the 1965- to 1980-cm^{-1} range (9, 26).

Our interpretations of the structural origins of the ν(CO) frequencies suggest that comparable effects should be observed for the binding of other bulky ligands. In this respect it is of interest to note that the orientation of the g_{zz} component of the g matrix of the spin hamiltonian of paramagnetic low-spin ferric complexes in crystals differs by ≈3–6° from that of high-spin ferric complexes (27), although no comparable changes in the positions of the peripheral porphyrin atoms are detected through difference Fourier (28) or polarized optical (10, 25) studies. Because the principal directions of the g matrix are determined by the immediate coordination environment of the iron, these results indicate that the iron–nitrogen bonding relationships must differ with respect to the heme axis that is perpendicular to the plane of peripheral porphyrin atoms.

¶ Substitution of the heme–carbonyl coordinates of MbCO (B. P. Schoenborn and J. C. Hanson, personal communication) for those of the porphyrin ring of metMb (12) and deoxyMb (13) was carried out by visual superposition of the corresponding average planes of the porphyrin ring with computer-assisted molecular graphics techniques (17). Superposition of the porphyrin rings is required by the observations that the direction cosines of the normal to the porphyrin plane in metMb and deoxyMb in the monoclinic crystal are identical (12, 13) and the Soret polarization ratios (25) of the orthorhombic MbCO, metMb, and deoxyMb crystals (refs. 10, 11; unpublished observations) indicate a difference of no more than 1.5° in heme tilt. This approach was sufficient to assess changes in the relative position of the distal (E7) histidine residue with respect to the iron–carbonyl group. Evaluation of changes in the relative orientations of the pyrrole nitrogen atoms and of the proximal (F8) histidine with respect to the iron–carbonyl unit requires separate consideration of the detailed environment of the nitrogen donor ligand atoms to the iron as described in crystallographic studies (12, 13).

These differences are readily accounted for by changes in the iron–nitrogen bonding relationships as illustrated in Fig. 3. It has been suggested (29) that the off-axis binding of the anionic cyanide ligand to the ferric iron in metHb may arise similarly through the deformability of the pyrrole nitrogen plane. This configuration of bound ligands may be a constraint of the heme crevice, because the results of potential energy calculations of Case and Karplus (30) indicate that configurational changes of side chains in the heme environment are more likely to result in tilt of a linear (Fe—Ĉ—O) unit from the heme normal rather than bending of the (Fe—Ĉ—O) valence angle.

Because the relative proportions of the 1933 and 1967 cm^{-1} components are increased in crystals by the presence of deoxyMb, it is of interest to note that the results of these investigations suggest that structural changes in the immediate environment of the heme–carbonyl group may occur as a function of the occupancy of ligand-binding sites. A variety of studies have been reported in which the ligand-binding properties of crystalline enzymes and proteins are modified through nonspecific intermolecular interactions induced by molecular packing relationships in the crystal (31). In a comparable manner, small differences in stereochemical relationships of protein–ligand interactions may be dependent upon the occupancy of binding sites by inhibitors, substrates, and effector molecules. Although such differences may account for no more than a few tenths of an ångstrom in the separation of atoms in nonbonding relationships, they may be important in discerning catalytic from nonproductive binding configurations of substrates and active site residues. The results of this study, thus, underline the subtle importance of these configurational changes in the evaluation of enzyme–substrate interactions through crystallographic studies.

We thank Mr. R. J. Feldmann of the National Institutes of Health for valuable assistance in model building studies and Drs. B. P. Schoenborn, J. C. Hanson, and T. Takano for providing listings of the refined atomic coordinate data of Mb. This work was supported by grants awarded to M.W.M. by the National Science Foundation (BCM 77-17648) and the American Heart Association (77873) and by a grant awarded to W.S.C. by the National Institutes of Health (HL 15980). M.W.M. is an Established Investigator of the American Heart Association.

1. Huber, R., Epp, O. & Formanek, H. (1970) *J. Mol. Biol.* **52** 349–354.
2. Heidner, E. J., Ladner, R. C. & Perutz, M. F. (1976) *J. Mol. Biol.* **104,** 707–722.
3. Norvell, J. C., Nunes, A. C. & Schoenborn, B. P. (1975) *Science* **190,** 568–570.
4. Tucker, P. W., Phillips, S. E. V., Perutz, M. F., Houtchens, R. A. & Caughey, W. S. (1978) *Proc. Natl. Acad. Sci. USA* **75,** 1076–1080.
5. Padlan, E. (1968) Dissertation (The Johns Hopkins University, Baltimore, MD).
6. Peng, S. M. & Ibers, J. A. (1976) *J. Am. Chem. Soc.* **98,** 8032–8036.
7. Hoard, J. L. (1975) in *Porphyrins and Metalloporphyrins,* ed. Smith, K. M. (Elsevier, Amsterdam), pp. 348–371.
8. McCoy, S. & Caughey, W. S. (1971) in *Probes of Structure and Function of Macromolecules and Membranes,* Probes of Enzymes and Hemoproteins, eds. Chance, B., Yonetani, T. & Mildvan, A. S. (Academic, New York), Vol. 2, pp. 289–291.
9. Alben, J. O. (1978) in *The Porphyrins,* ed. Dolphin, D. (Academic, New York), Vol. 3, Part A, pp. 323–345.
10. Churg, A. K. & Makinen, M. W. (1978) *J. Chem. Phys.* **68,** 1913–1925.
11. Churg, A. K., Danziger, R. S. & Makinen, M. W. (1978) in *Biochemical and Clinical Aspects of Hemoglobin Abnormalities,* ed. Caughey, W. S. (Academic, New York), pp. 323–331.
12. Takano, T. (1977) *J. Mol. Biol.* **110,** 537–568.
13. Takano, T. (1977) *J. Mol. Biol.* **110,** 569–584.
14. Kendrew, J. C. & Parrish, R. G. (1956) *Proc. Roy. Soc. (London)* **A238,** 305–324.
15. Maxwell, J. C. & Caughey, W. S. (1976) *Biochemistry* **15,** 388–396.
16. Maxwell, J. C. & Caughey, W. S. (1978) *Methods Enzymol.* **54,** 302–323.
17. Feldmann, R. J., Bing, D. H., Furie, B. C. & Furie, B. (1978) *Proc. Natl. Acad. Sci. USA* **75,** 5409–5412.
18. Choc, M. G. (1979) Dissertation (Colorado State University, Fort Collins, CO).
19. Yoshikawa, S., Choc, M. G., O'Toole, M. C. & Caughey, W. S. (1977) *J. Biol. Chem.* **252,** 5498–5508.
20. Rifkind, J. M., Keyes, M. H. & Lumry, R. (1977) *Biochemistry* **16,** 5564–5568.
21. Caughey, W. S., Houtchens, R. A., Lanir, A., Maxwell, J. C. & Charache, S. (1978) in *Biochemical and Clinical Aspects of Hemoglobin Abnormalities,* ed. Caughey, W. S. (Academic, New York), pp. 29–53.
22. Braterman, P. S. (1972) *Struct. Bonding* **10,** 57–86.
23. Braterman, P. S. (1976) *Struct. Bonding* **26,** 1–42.
24. Jetz, W. & Graham, W. A. G. (1967) *J. Am. Chem. Soc.* **89,** 2773–2775.
25. Makinen, M. W. & Eaton, W. A. (1974) *Nature* **247,** 62–64.
26. Alben, J. O. & Caughey, W. S. (1968) *Biochemistry* **7,** 175–183.
27. Hori, H. (1971) *Biochim. Biophys. Acta* **251,** 227–235.
28. Makinen, M. W. (1975) in *Techniques and Topics in Bioinorganic Chemistry,* ed. McAuliffe, C. A. (Macmillan, London), pp. 1–106.
29. Deatherage, J. F., Loe, R. S., Anderson, C. M. & Moffat, K. (1976) *J. Mol. Biol.* **104,** 687–706.
30. Case, D. A. & Karplus, M. (1978) *J. Mol. Biol.* **123,** 697–701.
31. Makinen, M. W. & Fink, A. L. (1975) *Annu. Rev. Biophys. Bioeng.* **6,** 301–343.